



Get Clarity On Generics

Cost-Effective CT & MRI Contrast Agents

 FRESENIUS
KABI

WATCH VIDEO

AJNR

Dose Reduction While Preserving Diagnostic Quality in Head CT: Advancing the Application of Iterative Reconstruction Using a Live Animal Model

F.D. Raslau, E.J. Escott, J. Smiley, C. Adams, D. Feigal, H. Ganesh, C. Wang and J. Zhang

This information is current as of August 6, 2025.

AJNR Am J Neuroradiol 2019, 40 (11) 1864-1870

doi: <https://doi.org/10.3174/ajnr.A6258>

<http://www.ajnr.org/content/40/11/1864>

Dose Reduction While Preserving Diagnostic Quality in Head CT: Advancing the Application of Iterative Reconstruction Using a Live Animal Model

 F.D. Raslau,  E.J. Escott,  J. Smiley,  C. Adams,  D. Feigal,  H. Ganesh,  C. Wang, and  J. Zhang

ABSTRACT

BACKGROUND AND PURPOSE: Iterative reconstruction has promise in lowering the radiation dose without compromising image quality, but its full potential has not yet been realized. While phantom studies cannot fully approximate the subjective effects on image quality, live animal models afford this assessment. We characterize dose reduction in head CT by applying advanced modeled iterative reconstruction (ADMIRE) in a live ovine model while evaluating preservation of gray-white matter detectability and image texture compared with filtered back-projection.

MATERIALS AND METHODS: A live sheep was scanned on a Force CT scanner (Siemens) at 12 dose levels (82–982 effective mAs). Images were reconstructed with filtered back-projection and ADMIRE (strengths, 1–5). A total of 72 combinations (12 doses \times 6 reconstructions) were evaluated qualitatively for resemblance to the reference image (highest dose with filtered back-projection) using 2 metrics: detectability of gray-white matter differentiation and noise-versus-smoothness in image texture. Quantitative analysis for noise, SNR, and contrast-to-noise was also performed across all dose-strength combinations.

RESULTS: Both qualitative and quantitative results confirm that gray-white matter differentiation suffers at a lower dose but recovers when complemented by higher iterative reconstruction strength, and image texture acquires excessive smoothness with a higher iterative reconstruction strength but recovers when complemented by dose reduction. Image quality equivalent to the reference image is achieved by a 58% dose reduction with ADMIRE-5.

CONCLUSIONS: An approximately 60% dose reduction may be possible while preserving diagnostic quality with the appropriate dose-strength combination. This in vivo study can serve as a useful guide for translating the full implementation of iterative reconstruction in clinical practice.

ABBREVIATIONS: ADMIRE = advanced modeled iterative reconstruction; CNR = contrast-to-noise ratio; FBP = filtered back-projection; IR = iterative reconstruction

Iterative reconstruction (IR), in requiring less radiation to produce diagnostic images, plays a central role in dose reduction while maintaining image quality.^{1,2} Although IR has been widely adopted, its full implementation is yet to be realized. It is our observation that hesitation in using the highest IR strengths is mainly due to overly “smooth” or “plastic” image texture that is deemed undesirable by radiologists. Image noise and texture characteristics reconstructed in a statistically optimal fashion

could be rather different from those of filtered back-projection (FBP). The traditional FBP reconstruction algorithm is analytic in nature. The relationship between radiation dose and perceived image quality is well known—that is, image noise is inversely proportionate to the square root of the radiation dose. However, IR algorithms are nonlinear in nature, so the use of low radiation does not necessarily translate into high image noise. In addition, the application of IR may push noise texture toward the lower frequency of the Fourier spectrum, resulting in a plastic appearance in the presented images.³ It is our contention that further dose reduction can be achieved without sacrificing image quality, but optimal imaging parameters must be established because various combinations influence the balance of image quality and radiation dose.⁴

Protocol optimization has traditionally turned to anthropomorphic phantoms⁴⁻¹³ and clinical patients.¹⁰⁻²¹ However, they have advantages and limitations. Phantoms (and cadavers) allow

Received July 5, 2019; accepted after revision August 21.

From the Departments of Radiology (F.D.R., E.J.E., C.A., D.F., H.G., J.Z.), Neurology (F.D.R.), Neurosurgery (F.D.R.), Otolaryngology-Head and Neck Surgery (E.J.E.), Laboratory Animal Resources (J.S.), and Biostatistics (C.W.), University of Kentucky, Lexington, Kentucky.

Paper previously presented as an electronic scientific poster at: Annual Meeting of the American Society of Neuroradiology, May 18–23, 2019; Boston, Massachusetts.

Please address correspondence to Flavius D. Raslau, MD, University of Kentucky, 800 Rose St, Lexington, KY 40536; e-mail: flavius.raslau@uky.edu

<http://dx.doi.org/10.3174/ajnr.A6258>

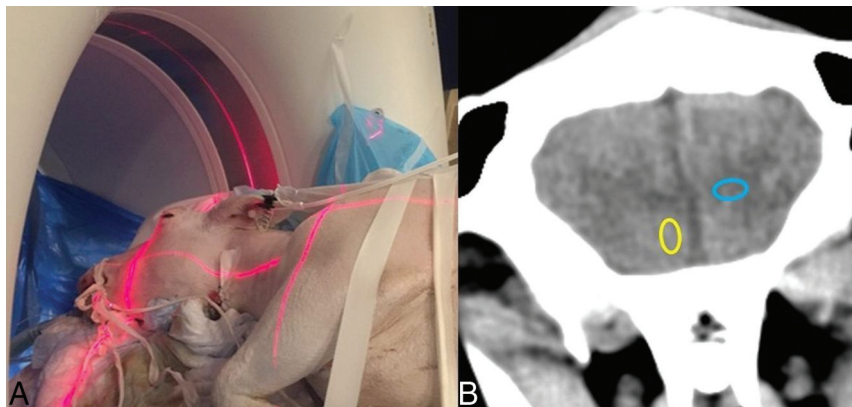


FIG 1. A, Positioning of the sheep, a 4-year-old 72-kg hornless white Dorper ewe, in the CT scanner. B, Sample coronal head CT images with ROIs marking the cortical gray matter (yellow) and deep white matter (blue) for quantitative analysis.

convenient repeatable testing under controlled conditions and additionally provide an objective metric for lesion detectability, which has emerged as an important metric in IR optimization.⁵⁻⁹ Even so, phantom studies are limited in that they fail to adequately reproduce the complexities of living tissue (eg, gray-white matter differentiation). Clinical trials are indispensably valuable, but this approach fails to control for many potential variables. Unwarranted radiation exposure should be avoided; therefore, only a narrow range of parameters can be tested and usually between follow-up scans separated by time.

Live animal studies provide a crucial bridge that can leverage advantages from both sides. Despite the virtues of such a middle-of-the-road approach, it is a path rarely trodden. Sparse studies have used pig²² brain with IR as well as dog²³ and pig²⁴ brains unrelated to IR, yet these animals were euthanized at the time of scanning, which alters physiology and calls into question their adequacy. Only in vivo models can adequately simulate the real-life concerns of practicing radiologists. Thus, live animal studies can help close the gap between the knowledge learned from anthropomorphic phantoms and its translation into clinical practice.

Advanced modeled iterative reconstruction (ADMIRE), which is made available by Siemens on their high-end CT scanners, is a model-based iterative reconstruction algorithm with more advanced noise-reduction methods. Our preliminary observations suggest that higher IR strengths require an appropriate choice of radiation exposure to mitigate the unwanted smoothing texture.²⁵ Moreover, the fact that image-quality assessment must scrutinize image texture is another point often neglected, which we wish to bring to the forefront. The purpose of this study was to characterize dose reduction in head CT by applying ADMIRE in a live ovine model, while evaluating preservation of gray-white matter detectability and image texture compared with the FBP reference.

MATERIALS AND METHODS

Animal Subject

This study was reviewed and approved by the University of Kentucky Institutional Animal Care and Use Committee and conducted in accordance with principles in the National

Research Council, 2011, *Guide for the Care and Use of Laboratory Animals*. 8th ed. Washington DC: National Academic Press.

The animal used for the study was a 4-year-old, 72-kg, hornless, white Dorper ewe procured from the University of Kentucky Research Sheep Center, Department of Food and Animal Sciences. The ewe was a cull breeding animal scheduled to be removed from the flock due to the loss of an udder to mastitis (condition resolved at time of the study).

Before transfer to the University of Kentucky Division of Laboratory Animal Resources facilities, negative pregnancy and Q fever statuses were

confirmed. The Division of Laboratory Animal Resources Experimental Surgery staff and a veterinarian oversaw anesthesia induction, monitoring, and animal transport. The animal fasted overnight and was induced with a mixture of midazolam (0.4 mg/kg, IV) + ketamine (5.5 mg/kg, IV) and orotracheal intubated and maintained on isoflurane (1.75%–2.0%) in 100% O₂ with breathing self-regulated. Isotonic crystalloid (0.9% NaCl, 5–10 mL/kg/h) was administered for the duration of the study. At the conclusion of imaging, the animal was euthanized by sodium pentobarbital overdose while remaining under anesthesia.

Scanning Protocol

Images were obtained on a Force CT scanner (Siemens, Erlangen, Germany). The sheep was in a lateral decubitus position in the gantry for the acquisition of coronal sections of the head (Fig 1A). Considering the morphology of the animal brain, the coronal section was chosen for optimal presentation and discrimination of cortical gray matter versus subcortical white matter. The FOV was 142 × 142 mm, and the matrix was 512 × 512, yielding 0.28 × 0.28 in-plane spatial resolution and a 5-mm section thickness. Tube voltage was fixed at 120 kV, pitch at 0.55, and row collimation at 0.6 mm. Tube current was varied from 982 to 82 effective mAs in 12 levels, with approximately 8% dose reduction between each level. Automated exposure control was turned off to control tube current in each run.

A standard protocol does not exist for scanning a small brain, weighing just 10% of the weight of a normal adult human brain. The application of automated exposure control to establish the starting reference dose did not produce adequate gray-white matter differentiation by the judgment of 2 neuroradiologists. The algorithm, which relies on a topogram-based calculation, likely failed due to the animal's disproportionately large face. Thus, the tube current for the reference protocol was identified by raising the tube current until the 2 neuroradiologists were satisfied with the diagnostic image quality and gray-white differentiation. Reconstruction algorithms performed at each dose level included FBP and ADMIRE IR strengths 1–5. A total of 72 combinations were generated by 12 dose levels × 6 reconstruction levels.

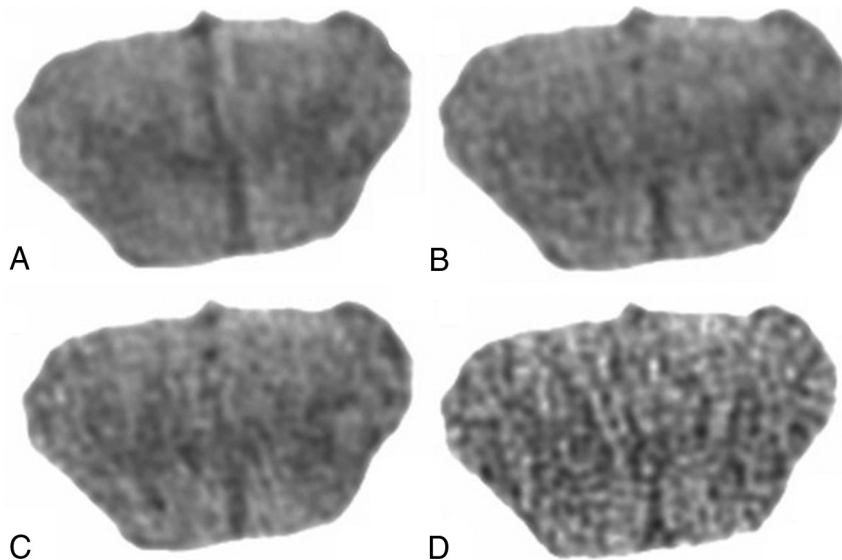


FIG 2. Benchmark coronal head CT images for rating scales of gray-white differentiation: 982 mAs with FBP for score = 4 (A), 573 mAs with FBP for score = 3 (B), 327 mAs with FBP for score = 2 (C), and 82 mAs with FBP for score = 1 (D).

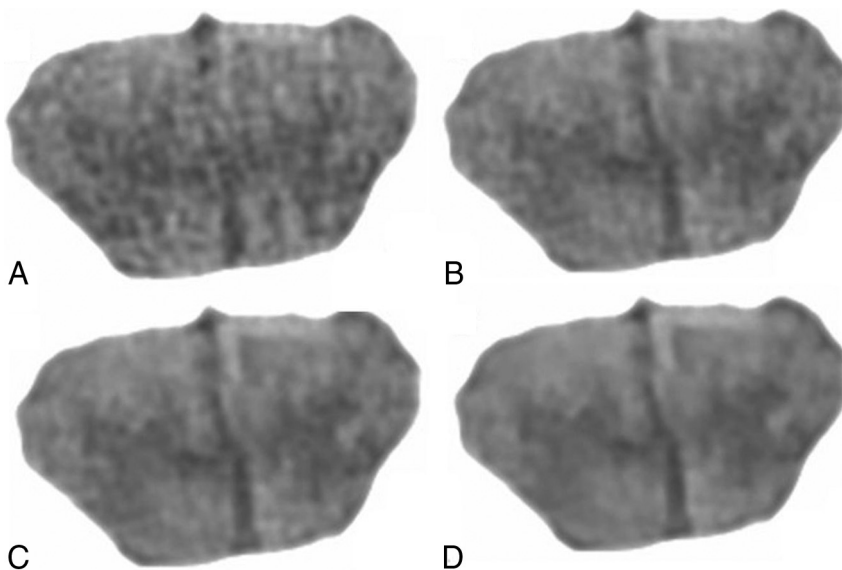


FIG 3. Benchmark coronal head CT images for rating scales of image texture: 409 mAs with FBP for score = 4 (A), 982 mAs with FBP for score = 3 (B), 982 mAs with ADMIRE-3 for score = 2 (C), and 982 with ADMIRE-5 for score = 1 (D).

Image Evaluation

One coronal section was chosen for evaluation on the basis of the criterion of maximizing the display of gray-white matter differentiation. All 72 images were anonymized in terms of technical and reconstruction factors and randomized and then evaluated on a standard PACS station. Both qualitative and quantitative measures were performed.

Qualitative ratings were made by 2 neuroradiologists (with 24 and 7 years' experience), who were blinded to all imaging parameters. They rated two 4-point metrics of image quality, gray-white matter differentiation and image texture: in the case of gray-white matter differentiation, 4 = distinct, 3 = regionally

decreased, 2 = globally decreased, 1 = indistinguishable; in the case of image texture: 4 = excessive pixilation (ie, noisy), 3 = balanced pixilation and smoothing, 2 = increased smoothing, 1 = excessive smoothing. Benchmark sample images were assigned to each score of the rating scale to restrict subjectivity on the part of the qualitative assessment; for the gray-white rating scale: 982 effective mAs with FBP for score = four, 573 effective mAs with FBP for score = three, 327 effective mAs with FBP for score = two, and 82 effective mAs with FBP for score = 1 (Fig 2). For the texture-rating scale, the scores were the following: 409 effective mAs with FBP for score = four, 982 effective mAs with FBP for score = three, 982 effective mAs with ADMIRE-3 for score = two, 982 effective mAs with ADMIRE-5 for score = 1 (Fig 3). The default score of the reference image (highest dose with FBP) was 4 for gray-white and 3 for texture, yielding a maximum combined score of 7 (Note that a rating of 4 in texture is suboptimal; therefore, it had to be reclassified as 2, thereby allowing the optimal middle-of-the-road texture to contribute to the highest score in simple algebraic combined scoring). All 72 randomized images were evaluated by matching the closest image on the rating scales. The scores by the 2 neuroradiologists were averaged. Heat maps were generated for gray-white, texture, and combined scores.

Quantitative analysis was also performed. Using a self-developed Matlab script (MathWorks, Natick, Massachusetts), an ROI was marked on 1 image and automatically reproduced on all other images of the same size

and in the same location. Two samples were taken, one centered in the cerebral cortical gray matter and another in the deep white matter (Fig 1B). Mean and SD values were recorded for each ROI. From these values, we calculated the noise and SNR of the white matter as well as contrast-to-noise ratio (CNR) of the cortex:

$$\text{Noise}_{\text{wm}} = \text{SD}_{\text{wm}}$$

$$\text{SNR}_{\text{wm}} = \text{mean}_{\text{wm}} / \text{SD}_{\text{wm}}$$

$$\text{CNR}_{\text{cortex}} = (\text{mean}_{\text{cortex}} - \text{mean}_{\text{wm}}) / \text{SD}_{\text{wm}}$$

Graphs were plotted to demonstrate the relationship among image quality, radiation dose, and reconstruction algorithm.

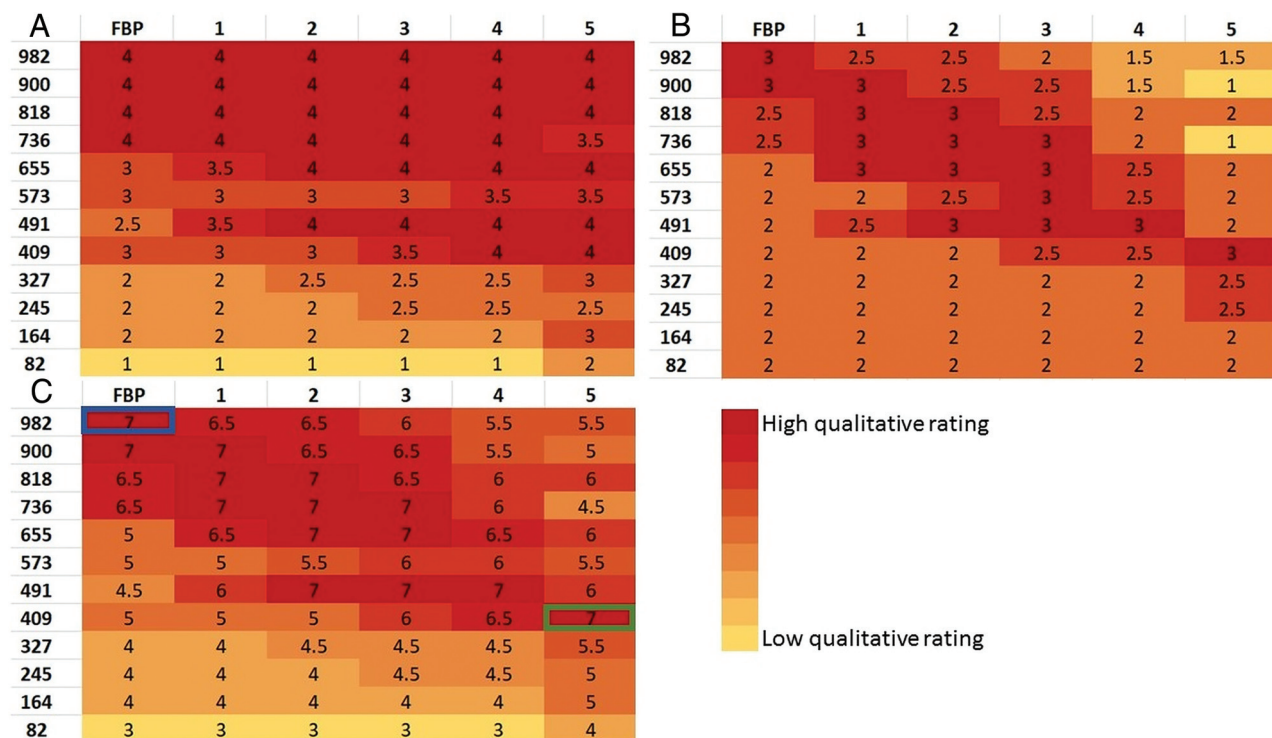


FIG 4. Heat maps of qualitative ratings of gray-white differentiation (A), image texture (B), and combined scores (C). Note that scores of 2 in the bottom left corner of the texture heat map were reclassified from original scores of 4 as explained in the Materials and Methods section. Most important, the low scores in the top right corner of texture heat map reveal the inadequacy of the high-dose and high-strength combination. The greatest dose reduction (58%) that preserves comparable gray-white differentiation and texture to the reference FBP (blue outline) is achieved at 409 mAs with ADMIRE-5 (green outline).

Statistical Analysis

Interneuroradiologist agreement was assessed using the weighted κ , which quantifies the agreement between the 2 neuroradiologists, adjusting for random chance and weighting by the degree of disagreement.

RESULTS

Heat maps of the qualitative rating of gray-white matter differentiation, image texture, and combined score reveal a distinct pattern. The highest score for gray-white matter differentiation (Fig 4A) is found with higher radiation doses across every reconstruction algorithm. Distinct gray-white matter differentiation was preserved at low radiation doses but only when using higher IR strengths.

The image texture heat map (Fig 4B) confirms that the combination of high radiation dose and high IR strength creates the smoothing texture. However, at lower radiation doses, with which noisy images would have been generated with FBP, higher IR strengths recover the normal image texture.

The heat map of the combined scores (Fig 4C) reveals optimal image quality along a diagonal, so that high dose levels with FBP, mid-dose levels with mid-IR strengths, and low-dose levels with high IR strengths produce images with gray-white matter differentiation and texture comparable with the reference image. According to this qualitative assessment, a 58% dose reduction can be achieved with ADMIRE-5 without compromising gray-white matter differentiation or image texture (see Fig 5 for sample images).

The quantitative analysis also reveals the effects of radiation dose and iterative strength on the noise of the white matter, SNR of the white matter, and CNR of the cortex (Fig 6). Noise, SNR, and CNR all improve with higher IR strength but worsen with dose reduction. Noise, SNR, and CNR equivalent to the reference image (ie, highest dose with FBP) can be maintained with a maximum of 67% dose reduction if the highest IR strength is used. Figure 6D further demonstrates the relationship between radiation dose and iterative strength. For any given reconstruction technique, CNR will drop when lowering the radiation dose, but it can be recovered by switching to higher iterative strengths. Therefore, the correct combination of dose reduction and higher iterative strength can preserve image quality. According to the quantitative analysis, 67% dose reduction can be achieved with ADMIRE-5, which is comparable with the independent results of the qualitative analysis.

Qualitative ratings made by 2 neuroradiologists showed very good agreement on both gray-white differentiation (weighted $\kappa = 0.91$) and image texture (weighted $\kappa = 0.84$).

DISCUSSION

While CT is indispensable for patient management, its contribution to radiation exposure and its potential for cancer induction has come under scrutiny.²⁶⁻²⁸ There are dueling incentives to both produce high quality imaging and reduce radiation exposure. Toward this end, our application of an in vivo model simultaneously achieves 2 critical experimental approaches: 1) to explore the full range of tube current and IR strengths, thus

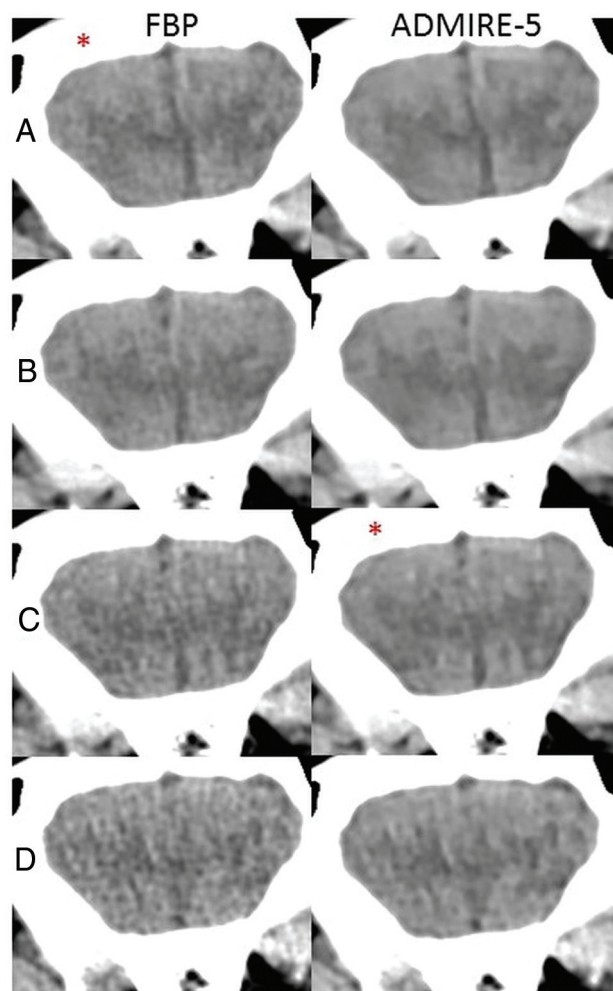


FIG 5. Sample coronal head CT images comparing FBP (left column) and ADMIRE-5 (right column) at the reference dose (A), 8% dose reduction (B), 58% dose reduction (C), and 75% dose reduction (D). Gray-white detectability and image texture were subjectively scored as equivalent between the reference dose with FBP (left, A) and a 58% dose reduction with ADMIRE-5 (right, C) as marked with an asterisk.

leveraging the advantage of phantom studies; and 2) to reproduce realistic gray-white matter differentiation, thus leveraging the advantage of clinical studies.

The search for an appropriate animal proxy faced several challenges. First, although apes would have offered the most comparable brains, the National Institutes of Health no longer supports biomedical research on apes for ethical considerations. Other animals with relatively large brains have prohibitively large bodies (eg, horse) or require specialized housing facilities (eg, California sea lion), and most other available animals have brains that are much too small (eg, macaque monkey). The sheep can serve as a suitable research subject for several reasons: Its body weight (72 kg in our subject) is acceptable for handling while anesthetized, it is widely available in agricultural centers, and its acceptability for human consumption renders the choice less ethically controversial. The ovine brain has garnered research interest in several areas, including functional cortical mapping,²⁹ modeling Huntington disease³⁰ and other neurodegenerative diseases,³¹ and evaluating surgical techniques.³² Calvarial thickness is

6 mm,³² which is comparable with that of the human skull, whereas the pig skull is much thicker.³³ Even so, the sheep brain is modest in size, weighing only 120–140g,²⁹ which is a mere 10% of an adult human brain and even less than half of that of a neonate.³⁴ In addition, the animal has a disproportionately large snout and masticator apparatus, which may be expected to attenuate x-rays and potentially interfere with image reconstruction of the brain. Despite these caveats, the sheep is a suitable animal model.

The present study advances our understanding of the application of IR technology. Early studies, including of the brain, tended to conclude, in glowing terms, that IR successfully achieves dose reduction while preserving image quality.^{10–18} Despite these bullish pronouncements, practicing radiologists have remained resistant to the full implementation of this technology. The facts of decreased noise, increased CNR, and qualitative ratings of noise and diagnostic acceptability were not capturing the whole story because it is well-known that radiologists hesitate to use high IR strengths due to a dissatisfaction with the generated images. A factor that merits more attention is that higher IR strengths introduce textural changes, which have been called blotchy, plastic, or smoothing in the literature. These textural effects are unfamiliar to radiologists and are perceived to cause decreased image quality and therefore are thought to produce inferior diagnostic quality. We created a 4-point rating scale that recognizes too noisy as being problematic on one end but also too smooth as being undesirable on the other end. We believe this noise-versus-smoothness metric will be sensitive to a principal reason that practicing radiologists are reticent to adopt the full implementation of IR technology.

While quantitative analysis suggested that a 67% dose reduction should be achievable without compromising image quality, qualitative evaluation concluded that only a 58% dose reduction is possible. If the degree of dose reduction were based on quantitative factors alone using SNR and CNR criteria, radiologists may not be comfortable with the generated image quality. These differential results advise caution and argue for the added value of qualitative metrics such as gray-white detectability and textural smoothness.

A second design feature that was specifically aimed at the concerns of practicing radiologists is to use resemblance to the reference FBP image as a pragmatic metric for assessing IR-rendered quality. Radiologists are already accustomed to the overall appearance and texture of FBP images; therefore, any replacement that might be rated subjectively equivalent would need to most resemble what is currently already widely in use. Therefore, the rating scale was benchmarked to preselected images and viewed at the time of qualitative assessment for the goal of identifying gray-white differentiation for low-contrast detectability and image texture that most closely resembled the reference image.

Our study surveyed a range of dose-strength combinations and found that lower doses and higher IR strengths must be properly paired for the preservation of image quality. If the dose is not low enough for the chosen IR strength or the IR strength is not high enough for the desired dose reduction, image quality may suffer. Below a certain dose, no level of IR strength can recover image quality. Our study suggests that up to 60% dose

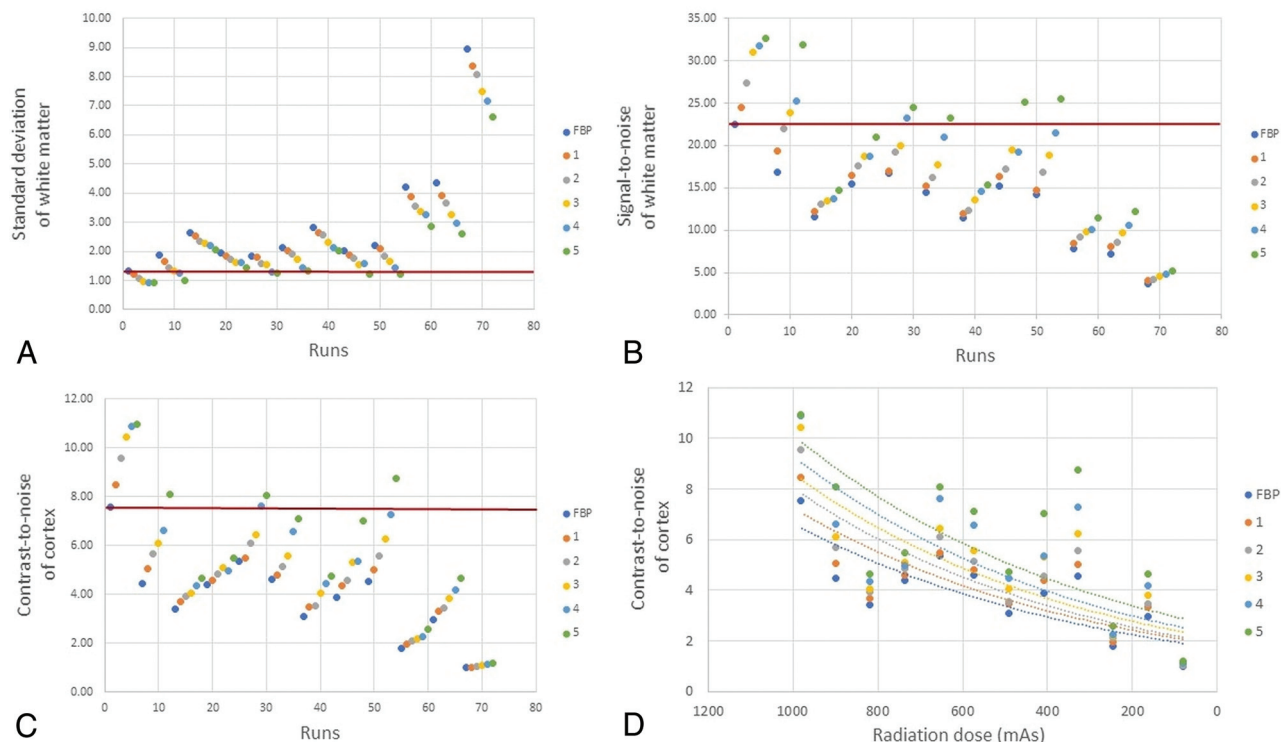


FIG 6. SD (ie, noise) of the white matter (A), signal-to-noise of the white matter (B), and contrast-to-noise of the cortex (C) for each run, from the highest (982 mAs) to lowest (82 mAs) effective dose; FBP followed by ADMIRE 1–5 for each dose level. Noise, SNR, and CNR all improve with higher IR strength but worsen with dose reduction. Noise, SNR, and CNR equivalent to the reference image (ie, highest dose with FBP) as illustrated by red horizontal line can be maintained with a 67% dose reduction at the highest IR strengths. Equivalent noise, SNR, and CNR cannot be preserved at further dose reductions regardless of IR strength. The last graph (D) relates CNR of the cortex to the radiation dose for each reconstruction technique. In each case, the CNR decreases with progressive dose reduction. However, for any given radiation dose, higher IR strengths improve the CNR. If the CNR is to be preserved, dose reduction must be complemented by higher IR strength.

reduction may be achieved in brain imaging with appropriate dose-strength combinations.

A limitation of our study is that results apply only to ADMIRE, which is Siemens' most advanced IR algorithm available on their newest scanners. Because IR algorithms work differently and possess different profiles of advantages and disadvantages,^{6–8,35} how these results translate to other techniques is not well-understood. This study also did not evaluate the impact of varying spatial resolution. Different from FBP, IR does not have the sharpness-noise trade-off limitation. In other words, an equivalent noise profile could be produced at a higher spatial resolution setting.³⁶ Another concern is that only 1 subject was included in this study. A limitation of this (and every) study is that dose reduction is dependent on the starting reference FBP dose. It is not entirely clear how our starting reference dose in the sheep (though appropriately chosen for its small brain and disproportionately large face) might translate to the proportions of the human brain. These preliminary results require additional larger trials using multiple vendors, and clinical validation is necessary.

CONCLUSIONS

IR has promise in lowering radiation exposure without compromising image quality, but its full implementation has not yet been reached. The present study uses an in vivo animal model, which

affords assessment of the full range of tube current and ADMIRE strengths in the living brain. Qualitative assessment of low-contrast detectability and image texture for resemblance to the reference FBP image suggests that an approximately 60% dose reduction is achievable with ADMIRE-5.

Disclosures: Jeffrey Smiley—*UNRELATED: Employment:* University of Kentucky. Jie Zhang—*UNRELATED: Grants:* National Institutes of Health, R21, *Comments:* This is a research grant from the National Institutes of Health, R21, and I am a coinvestigator with 4% effort*; *Payment for Development of Educational Presentations:* Radiological Society of North America physics module revision, *Comments:* We are revising the Radiological Society of North America physics module gamma camera.* *Money paid to the Institution.

REFERENCES

- Geyer LL, Schoepf UJ, Meinel FG, et al. **State of the art: iterative CT reconstruction techniques.** *Radiology* 2015;276:339–57 [CrossRef](#) [Medline](#)
- Padole A, Khawaja RDA, Kalra MK, et al. **CT radiation dose and iterative reconstruction techniques.** *AJR Am J Roentgenol* 2015;204:W384–92 [CrossRef](#) [Medline](#)
- Ghetti C, Palleri F, Serreli G, et al. **Physical characterization of a new CT iterative reconstruction method operating in sinogram space.** *J Appl Clin Med Phys* 2013;14:434 [CrossRef](#) [Medline](#)
- Solomon J, Mileto A, Ramirez-Giraldo JC, et al. **Diagnostic performance of an advanced modeled iterative reconstruction algorithm for low-contrast detectability with a third-generation dual-source multidetector CT scanner: potential for radiation dose reduction in a multireader study.** *Radiology* 2015;275:735–45 [CrossRef](#) [Medline](#)

5. Schindera ST, Odedra D, Raza SA, et al. **Iterative reconstruction algorithm for CT: can radiation dose be decreased while low-contrast detectability is preserved?** *Radiology* 2013;269:511–18 [CrossRef Medline](#)
6. Mievil FA, Gudinchet F, Brunelle F, et al. **Iterative reconstruction methods in two different MDCT scanners: physical metrics and 4-alternative forced-choice detectability experiments: a phantom approach.** *Phys Med* 2013;29:99–110 [CrossRef Medline](#)
7. Jensen K, Martinsen ACT, Tingberg A, et al. **Comparing five different iterative reconstruction algorithms for computed tomography in an ROC study.** *Eur Radiol* 2014;24:2989–3002 [CrossRef Medline](#)
8. Love A, Olsson ML, Siemund R, et al. **Six iterative reconstruction algorithms in brain CT: a phantom study on image quality at different radiation dose levels.** *Br J Radiol* 2013;86:20130388 [CrossRef Medline](#)
9. Dobeli KL, Lewis SJ, Meikle SR, et al. **Noise-reducing algorithms do not necessarily provide superior dose optimisation for hepatic lesion detection with multidetector CT.** *Br J Radiol* 2013;86:20120500 [CrossRef Medline](#)
10. Vorona GA, Zuccoli T, Sutcliffe T, et al. **The use of adaptive statistical iterative reconstruction in pediatric head CT: a feasibility study.** *AJNR Am J Neuroradiol* 2013;34:205–211 [CrossRef Medline](#)
11. Baskan O, Erol C, Ozbek H, et al. **Effect of radiation dose reduction on image quality in adult head CT with noise-suppressing reconstruction system with a 256 slice MDCT.** *J Appl Clin Med Phys* 2015;16:285 [CrossRef Medline](#)
12. Singh S, Kalra MK, Hsieh J, et al. **Abdominal CT: comparison of adaptive statistical iterative and filtered back projection reconstruction techniques.** *Radiology* 2010;257:373–83 [CrossRef Medline](#)
13. Baker ME, Dong F, Primak A, et al. **Contrast-to-noise ratio and low-contrast object resolution on full- and low-dose MDCT: SAFIRE versus filtered back projection in a low-contrast object phantom and in the liver.** *AJR Am J Roentgenol* 2012;199:8–18 [CrossRef Medline](#)
14. Kilic K, Erbas G, Guryildirim M, et al. **Lowering the dose in head CT using adaptive statistical iterative reconstruction.** *AJNR Am J Neuroradiol* 2011;32:1578–82 [CrossRef Medline](#)
15. Korn A, Fenchel M, Bender B, et al. **Iterative reconstruction in head CT: image quality of routine and low-dose protocol in comparison with standard filtered back-projection.** *AJNR Am J Neuroradiol* 2012;33:218–24 [CrossRef Medline](#)
16. Alper S, Mohan P, Chaves I, et al. **Image quality and radiation dose comparison between filtered back projection and adaptive statistical iterative reconstruction in non-contrast head CT studies.** *OMICS J Radiol* 2013;2:7 [CrossRef](#)
17. Rapalino O, Kamalian S, Kamalian S, et al. **Cranial CT with adaptive statistical iterative reconstruction: improved image quality with concomitant radiation dose reduction.** *AJNR Am J Neuroradiol* 2012;33:609–15 [CrossRef Medline](#)
18. Brodoefel H, Bender B, Schabel C, et al. **Potential of combining iterative reconstruction with noise efficient detector design: aggressive dose reduction in head CT.** *Br J Radiol* 2015;88:20140404 [CrossRef Medline](#)
19. Iyama Y, Nakaura T, Oda S, et al. **Iterative reconstruction designed for brain CT: a correlative study with filtered back projection for the diagnosis of acute ischemic stroke.** *J Comput Assist Tomogr* 2017;41:884–90 [CrossRef Medline](#)
20. Kataria B, Althen JN, Smedby O, et al. **Assessment of image quality in abdominal CT: potential dose reduction with model-based iterative reconstruction.** *Eur Radiol* 2018;28:2464–73 [CrossRef Medline](#)
21. Pickhardt PJ, Lubner MG, Kim DH, et al. **Abdominal CT with model-based iterative reconstruction (MBIR): initial results of a prospective trial comparing ultralow-dose with standard-dose imaging.** *AJR Am J Roentgenol* 2012;199:1266–74 [CrossRef Medline](#)
22. Kim HJ, Lee HK, Song H, et al. **Reduction in radiation dose with reconstruction technique in the brain perfusion CT.** *Radiation Effects and Defects in Solids* 2011;166:918–26 [CrossRef](#)
23. Zarelli M, Schwarz T, Puggioni A, et al. **An optimized protocol for multislice computed tomography of the canine brain.** *Vet Radiol Ultrasound* 2014;55:387–92 [CrossRef Medline](#)
24. Zarb F, McEntee MF, Rainford L. **CT radiation dose and image quality optimization using a porcine model.** *Radiol Technol* 2013;85:127–36 [Medline](#)
25. Ge G, Zhang J. **Noise and texture properties for the optimization of CT protocols with iterative reconstruction algorithms.** In: *Proceedings of the Annual Meeting of American Association of Physicists in Medicine*, Nashville, Tennessee. July 29 to August 2, 2018
26. Pearce MS, Salotti JA, Little MP, et al. **Radiation exposure from CT scans in childhood and subsequent risk of leukaemia and brain tumours: a retrospective cohort study.** *Lancet* 2012;380:499–505 [CrossRef Medline](#)
27. Brenner DJ, Hall EJ. **Cancer risks from CT scans: now we have data, what next?** *Radiology* 2012;265:330–31 [CrossRef Medline](#)
28. Miglioretti DL, Johnson E, Williams A, et al. **Pediatric computed tomography and associated radiation exposure and estimated cancer risk.** *JAMA Pediatr* 2013;167:700–07 [CrossRef Medline](#)
29. John SE, Lovell TJH, Opie NL, et al. **The ovine motor cortex: a review of functional mapping and cytoarchitecture.** *Neurosci Biobehav Rev* 2017;80:306–15 [CrossRef Medline](#)
30. Handley RR, Reid SJ, Patassini S, et al. **Metabolic disruption identified in the Huntington's disease transgenic sheep model.** *Sci Rep* 2016;6:20681 [CrossRef Medline](#)
31. Oswald MJ, Palmer DN, Kay GW, et al. **Glial activation spreads from specific cerebral foci and precedes neurodegeneration in presymptomatic ovine neuronal ceroid lipofuscinosis (CLN6).** *Neurobiol Dis* 2005;20:49–63 [CrossRef Medline](#)
32. Laure B, Petraud A, Sury F, et al. **Resistance of the sheep skull after a monocortical cranial graft harvest.** *J Craniomaxillofac Surg* 2012;40:261–65 [CrossRef Medline](#)
33. Shridharani JK, Wood GW, Panzer MB, et al. **Porcine head response to blast.** *Front Neurol* 2012;3:70 [CrossRef Medline](#)
34. Dekaban AS. **Changes in brain weights during the span of human life: relation of brain weights to body heights and body weights.** *Ann Neurol* 1978;4:345–56 [CrossRef Medline](#)
35. Stiller W. **Basics of iterative reconstruction methods in computed tomography: a vendor-independent overview.** *Eur J Radiol* 2018; 109:147–54 [CrossRef Medline](#)
36. Mehta D, Bayraktar B. **Iterative reconstruction techniques for spatial resolution improvements: phantom study.** In: *Proceedings of the Annual Meeting of European Society of Radiology*. Vienna, Austria. March 3–7, 2011